Chapter 1

Introduction

1.1 Motivation

The stability of thin liquid films within various disperse systems is critical for people to better understand many industrial processes such as the mineral flotation and oil recovery operations. In froth flotation process, hydrophobic particles are collected on the surface of air bubbles and rise to the surface of an ore pulp to form a froth phase. The rate-determining step of flotation can be the stability of foams and froths (1-3). In the froth phase, bubbles laden with particles grow in size, and less strongly adhering particles drop off the bubble surface and are subsequently returned to the pulp phase. Thus, the froth phase provides a mechanism for removing the gangue minerals that are loosely held to the bubble surface. In column flotation, wash water is added to accelerate the process of removing the entrained particles. More and more flotation engineers recognize the importance of better understanding the physics and chemistry of froth and, thereby, improving the performance of their flotation cells. However, relatively little is known of the basic sciences involved in foam and froth and, therefore, it is difficult to model the froth behavior in flotation.

Also, many operators use stronger frothers to produce smaller air bubbles in order to increase the recovery of fine particles and, hence, higher recovery and throughput. Despite its importance, little is known of the fundamentals of foam and froth stability. Foam is a two-phase froth. The fundamental research on foam stability is expected to set a path to understanding of the stability of froths in the presence of solid particles.

The central theme of this research is to gain a better understanding of surface forces that arise in foam films confined between air bubbles, and how these forces affect the stability of three-dimensional foams.

1.2 Foam films

1.2.1 Charge of Air-Water Interface

Most substances carry an electric charge when immersed in polar liquid (e.g., aqueous solutions). Electrostatic surface charges (ζ-potential) of particles and bubbles play an important role in affecting flotation process. A usual way to determine the surface charges of these colloids is to measure their electrokinetic behavior in liquid by applying an external electrical field. The experimental methods to measure the ζ-potential of air bubbles have been reviewed by Graciaa et al (4). There are many difficulties associated with ζ-potential measurement of air bubbles. Among them are the generation of uniform microbubbles and the location of the stationary levels. It is accepted that air bubbles in pure water are negatively charged, based on the accumulated experimental results (5-12). However, no consensus has been reached upon the absolute values of ζ-potentials of air bubbles in pure water. Nevertheless, the trends reported in the literature are coherent for

the changes in ζ-potentials of air bubbles with changing pH, surfactant and electrolyte concentrations, respectively.

The origin of negative surface charges at the air/water interface is still not clear. The most probable explanation is a specific adsorption of OH^- ions (7, 13-16). The negative charge at air/water interface might also originate from interfacial water dipole moment (17-19). These investigators proposed a preferred orientation of the surface water dipole towards the bulk region. That is, the presence of both positive and negative ends of the water dipole at the free-water surface implies partial dipole moment cancellation, leaving the net negative component that one can measure.

1.2.2 Foam Film Structure and Types

The foam film, as a tool for the study of surface forces (e.g., double layer repulsion and van der Waals attractioin), has the advantage of its static equilibrium, well-defined geometry and reasonably well-known structure (20). It exhibits a huge degree of organization, and is therefore deemed as a model system in colloid and biological membrane science, in particular for the study of interface forces (21, 22).

Surfactants and electrolytes are often used to control the properties of foams and foam films. Based on the thickness (H) and the characteristic properties, the thin liquid film can be classified in the following types:

1) thick films (H >100 nm);
2) common black films (CBF) (10 nm < H < 60 nm);
3) Newton black films (NBF) (H <10 nm).

Usually thick films can be obtained at low electrolyte concentration where the electrostatic double layer force plays a dominant role, and the van der Waals force is negligible.

The NBF consists of a well-defined bilayer and an extremely thin water-layer of approximately 0.37 nm (21), and its stability is determined by hydration and/or entropic confinement forces (23, 24).

1.3 Disjoining pressure

1.3.1 Definition

The disjoining pressure was defined at mechanical equilibrium by Derjaguin and Churaev (25) as the difference existing between the pressure normal to the surface of a thin plane-parallel interface and the pressure in the adjacent bulk of the phase from which the film has been formed by thinning out. A typical symmetrical thin foam film is represented in Figure 1.1. The film thickness is denoted as H. There are several force balances,

$$\Pi(H) = P_{film} - P_{bulk} \quad [1.1]$$

$$P_{air} = P_{film} \quad [1.2]$$

$$P_{air} = P_{bulk} + P_c \quad [1.3]$$

from above equations, the disjoining pressure (Π) can be experimentally determined by the capillary pressure (P_c) at equilibrium:

$$\Pi = P_c \,. \qquad [1.4]$$

Note that a disjoining pressure is somewhat misleading in foam films in that attractive forces actually belong to a conjoining pressure. Therefore, repulsive forces are often called (positive) disjoining pressures, whereas attractive forces are negative disjoining pressures.

1.3.2 Thermodynamic definition

Eriksson and Toshev (26) introduced the Gibbs free energy of the film as $G^{f'}=F^{f}+P_{bulk}AH$, where F^{f} is the Helmholtz free energy of the film, A is the surface area, and H is film thickness. The corresponding Gibbs free energy differential is given by

$$dG^{f'} = -S^{f}dT + AHdP_{bulk} + 2\gamma^{fs}dA - \Pi AdH + \sum_i \mu_i dn_i^f \qquad [1.5]$$

where γ^{fs} is the film surface tension, S^{f} is the excess entropy of the two film interfaces, μ_i is chemical potentials of the ith component.

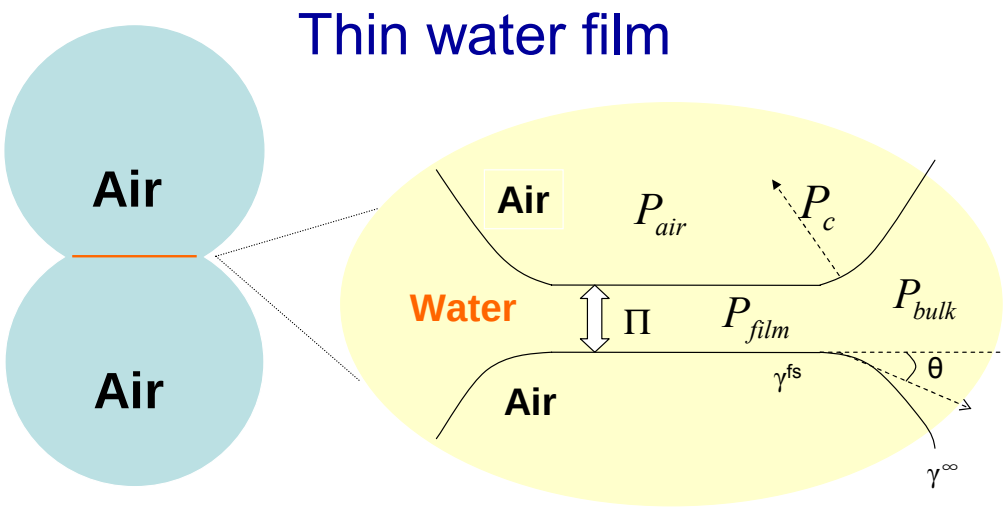

Figure 1.1 Schematic of a thin foam film.

The Derjaguin disjoining pressure can be thermodynamically defined by a change in the Gibbs free energy of the film (27),

$$\left(\frac{\partial(G^{f'}/A)}{\partial H}\right)_{T,P_{bulk},A,n_i^f} = -\Pi \qquad [1.6]$$

and the film surface tension, γ^{fs}, can be expressed by

$$\left(\frac{\partial G^{f'}}{\partial A}\right)_{T,P_{bulk},H,n_i^f} = \gamma^{fs} \qquad [1.7]$$

From integration of Eq. [1.5], Eriksson and Toshev derived the Gibbs-Duhem kind of equation:

$$-2d\gamma^{fs} = \left(\frac{S^f}{A}\right)dT - HdP_{bulk} + \Pi dH + \sum_i \Gamma_i^f d\mu_i \qquad [1.8]$$

From Eq. [1.8], one can see Π and γ^{fs} have the following relation,

$$2\left(\frac{\partial \gamma^{fs}}{\partial H}\right)_{T,\mu_2,\mu_3,P_{bulk}} = -\Pi \qquad [1.9]$$

where μ_2 and μ_3 are the chemical potentials of the surfactant and the salt, respectively. Thus, the disjoining pressure is twice the rate of change of γ^{fs} with H at constant state of the meniscus solution.

The thin liquid film is a third phase besides air phase and bulk aqueous phase, by integrating Eq. [1.9], the corresponding overall film tension at equilibrium is given by (27)

$$\gamma^f = 2\gamma^{fs} + \Pi H = 2\gamma^{\infty} - \int_{\infty}^{h} \Pi dh + \Pi H \qquad [1.10]$$

From Figure 1.1, one can readily see that $\gamma^{fs} = \gamma^{\infty}\cos\theta$, where θ is the contact angle at the Plateau border, and γ^{∞} is the surface tension of the meniscus. The contact angle can be experimentally determined, and it provides the interaction free energy of a film (27):

$$\Delta f(H) = -\int_{\infty}^{h} \Pi dH = 2\gamma^{\infty}(\cos\theta - 1) \qquad [1.11]$$

1.3.3 Components of the disjoining pressure

The classical Derjaguin-Landau-Verwey-Overbeek (DLVO) theory is commonly used to explain the stability of foams and foam films with varying degrees of success. It consists of the electrostatic double layer force and van der Waals force. For single soap films, discrepancies between DLVO theory and experiment have been repeatedly found (20, 28-30), indicating that the DLVO forces alone could not explain the results using the classical DLVO theory. It is now generally recognized that non-DLVO forces such as steric force, hydration force and hydrophobic force are also important in determining the stability of thin water films (23, 31-34). It is customary to assume that various contributions to the disjoining pressure are additive, one can use the following equation to express the surface forces in soap films:

$$\Pi = \Pi_{el} + \Pi_{vw} + \Pi_{hb} + \Pi_{hydration} + \Pi_{steric} + \cdots \qquad [1.12]$$

where Π_{el} is electric-double layer forces, Π_{vw} van der Waals forces, Π_{hb} hydrophobic force, $\Pi_{hydration}$ hydration force, Π_{steric} steric force (entropic confinement force). There might also be other forces, including supramolecular structuring forces (23).

Electrostatic Double Layer Forces

The charged surface and the neutralizing diffuse layer of counterions form an electrical double layer. There is a distribution of counterions between two planar charge surfaces. Figure 1.2 is a typical diagram for the ionic distribution. The reason why the counterions build up at each surface is simply because of their electrostatic repulsion and their entropy of mixing. The couterion concentration varies with distance, which can be calculated on the basis of Poisson-Boltzmann equation and Gouy-Chapman theory.

Based on the contact value theorem (35), the electrostatic double-layer interaction between charged surfaces in electrolyte is given by

$$\Pi_{el} = kT(\rho_m - \rho_\infty) \qquad [1.13]$$

which shows that Π_{el} is simply the excess osmotic pressure of the ions in the midplane over the bulk pressure. For a 1:1 electrolyte, one can have

$$\Pi_{el} = 2RTC_{el}\left(\cosh(\frac{e\psi_{mid}}{kT}) - 1\right) \qquad [1.14]$$

where C_{el} is electrolyte concentration, R the gas constant, e the electric charge, and ψ_{mid} the potential at the mid-plane of the film.

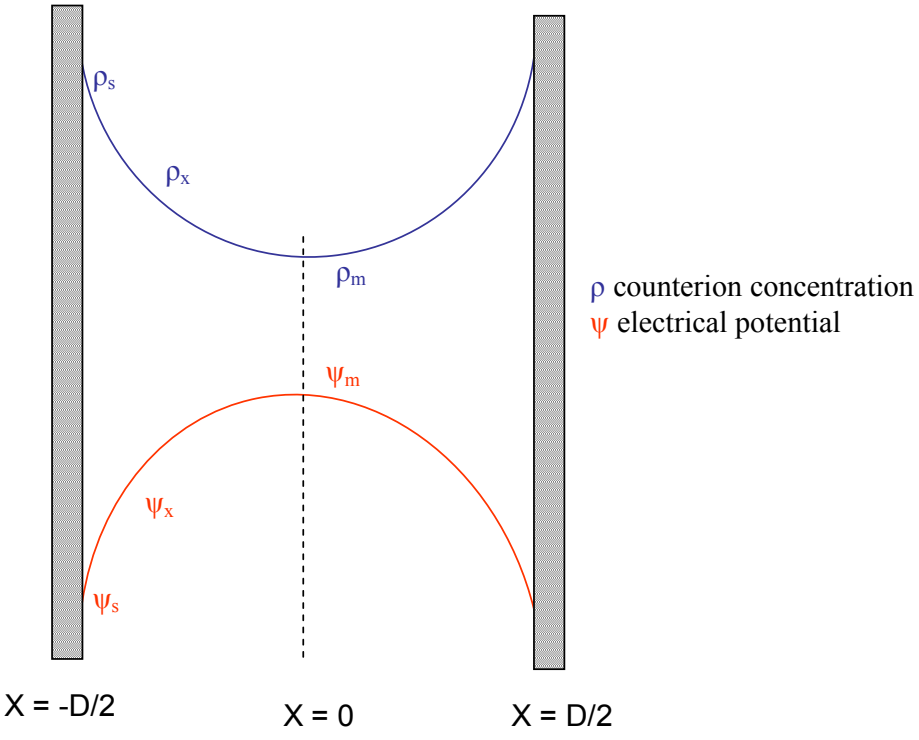

Figure 1.2. The counterion density and electrostatic potential with the aqueous region between two charged surfaces.

As the midplane potential ψ_m is very small and is assumed to be the sum of the potentials of each surface at x=½D as derived for an isolated surface, the weak overlap approximation for electrostatic force between two planar surfaces is given by

$$\Pi_{el} = 64 C_{el} RT \Gamma_0^2 \exp(-\kappa D) \qquad [1.15]$$

where

$$\Gamma_0 = \tanh\left(\frac{e\psi_s}{4kT}\right) \qquad [1.16]$$

where z is the valency, the Debye length (κ^{-1}) is given by (35)

$$\kappa^{-1} = \left(\frac{\varepsilon_r \varepsilon_0 kT}{2e^2 N_A I}\right)^{1/2} \qquad [1.17]$$

where ε_0 and ε_r are the permittivity of vacuum and the dielectric constant of water, respectively, and N_A is Avogadro's number. The Debye length is the characteristic length of the diffuse electric double layer. For 1:1 electrolytes (e.g., NaCl), $\kappa^{-1} = 0.304/C_{el}^{1/2}$ nm, when C_{el} is in unit of mole/liter. Obviously, the Debye length decreases as C_{el} increases, indicating that the electrostatic force becomes shorter range with adding electrolyte. Note that when the separation distance D falls into the regime of $\kappa D \leq 2$, the weak overlap approximation for electrostatic force (Eq. [1.15]) may not be applicable. Instead, one should use Eq. [1.14] to calculate the electrostatic force.

In the framework of Gouy-Chapman theory, the charge on a surface is assumed to be uniformly smeared out over the surface. And all the above equations are established on this base. In reality, however, this condition is hardly met with. Israelachvili (35) investigated the effects of discrete surface charges and dipoles, and found that at a position ½d (d is the distance between two neighboring charges) away from the surface, the electric field is up to 17% different from that the smeared-out field. For a bare air/water interface, ½d is estimated to be around 12 nm, from the surface charge density, which in turn is calculated using the Grahame equation from the zeta potential of air bubbles in pure water, -65 mV, at natural pH 5.6~5.8 (36). By changing the zeta potential from -30 to -80 mV, ½d varies from 20 to 10 nm. Therefore, the "discrete charge effect" in foam films at low surfactant and electrolyte concentrations might be significant.

van der Waals Dispersion Forces

The van der Waals dispersion forces are always present between two macroscopic bodies. In foam films, the van der Waals forces are attractive.

Microscopically, Hamaker (37) expressed the non-retarded van der Waals interaction free energies based on pairwise additivity. The Hamaker constant A_H is define as

$$A_H = \pi^2 C \rho_1 \rho_2 \qquad [1.18]$$

where ρ_1, ρ_2 are the number of atoms per unit volume in the two bodies and C is the coefficient in the atom-atom pair potential. For two parallel planes, the van der Waals disjoining pressure is given by

$$\Pi_{vw} = -\frac{A_{\mathrm{H}}}{6\pi D^3} \qquad [1.19]$$

Macroscopically, the Lifshitz theory (38) avoided the break-down problem of additivity, and provided an alternative way to calculate the Hamaker constant as follows:

$$A_{Total} = A_{\nu=0} + A_{\nu>0}$$

$$\approx \frac{3}{4}kT\left(\frac{\varepsilon_2-\varepsilon_3}{\varepsilon_2+\varepsilon_3}\right)^2 + \frac{3h_P\nu_e}{8\sqrt{2}}\frac{(n_1^2-n_3^2)(n_2^2-n_3^2)}{(n_1^2+n_3^2)^{1/2}(n_2^2+n_3^2)^{1/2}\left((n_1^2+n_3^2)^{1/2}+(n_2^2+n_3^2)^{1/2}\right)} \qquad [1.20]$$

where h_P is the Planck's constant (6.63×10^{-34} J·s), ν_e the main electronic adsorption frequency (3×10^{15} Hz), c the speed of light in a vacuum (3.0×10^{8} m/s), n_1 and n_2 refractive index of phases 1 and 2, respectively, n_3 refractive index of the solution, ε_2 dielectric constant of air, and ε_3 dielectric constant of water.

For the symmetric case of two air phases 2 interacting across medium 3, one can have

$$A_{232} = \frac{3}{4}kT\left(\frac{\varepsilon_2-\varepsilon_3}{\varepsilon_2+\varepsilon_3}\right)^2 + \frac{3h_P\nu_e}{16\sqrt{2}}\frac{(n_2^2-n_3^2)^2}{(n_2^2+n_3^2)^{3/2}} \qquad [1.21]$$

It is well known that at distances beyond about 5 nm the dispersion contribution to the total van der Waals force begins to decay rapidly because of electromagnetic retardation effects. If retardation effect is considered, Eq. [1.21] needs to be corrected with a coefficient, which is a function of separation distance. Typically, the Hamaker constant A_{232} is within the order of 10^{-20} J for foam films.

Hydrophobic Forces

Hydrophobic particles suspended in water attract with each other due to forces that are larger than the van der Waals forces, a process generally referred to as hydrophobic interaction (or force). For almost three decades, there have been going very active studies on hydrophobic force in thin aqueous films, such as wetting films (34, 39, 40) and thin aqueous films between two hydrophobized solid surfaces (41-47). The existence of a strong, *short-ranged* hydrophobic force has been convincingly verified, and its origin can readily be attributed to water restructuring occurring in the close vicinity of hydrophobic surfaces. However, the origin of the *long-ranged* hydrophobic force seems less clear. Different kinds of hydrophobic surface forces have been discussed and modeled, in particular: i) hydrogen-bond-propagated ordering of interfacial water molecules (41, 48); ii) bridging nano-bubbles of air between the hydrophobic surfaces (49). Moreover, a number of electrostatic interaction mechanisms have been subjected to

critical tests (50), and likewise the notion of thin air films being present on hydrophobic surfaces submerged in water (51). Yet, none of these alternative approaches have been found justifiable for the most ideal hydrophobic surfaces that one can prepare for which the hydrophobic attraction is maximized.

Although no general agreement on the origin of hydrophobic force has been reached, a straightforward and satisfactory explanation has been given by Eriksson et al (48), based on the water structure rearrangement induced by the surfaces. Israelachvili and McGuiggan (52) demonstrated schematically that the orientations of water molecules at the vicinity of hydrophobic and hydrophilic surface are quite different. Tangential alignment of water molecules exists near two hydrophobic surfaces, whereas normal alignment of water molecules exists at hydrophilic surfaces. Further, the water molecules near the hydrophilic surfaces are subject to the electrical field, and therefore the resulted anti-parallel orientation of water molecules at the mid-plane of the intervening aqueous film gives rise to repulsive solvation forces. Note that the water molecules beneath the first layer of water in direct contact with the hydrophobic surface will form a surface-induced network, in a cooperative fashion. The overall water structure rearrangement leads to the free energy gain (increased negativity) due to the enhanced hydrogen bond formation, which eventually causes the water film tension to diminish as the thickness shrinks (53). This is manifested as a hydrophobic attraction or a negative disjoining pressure.

Indeed, Eriksson and Yoon (53) integrated the experimental disjoining pressure isotherms obtained at different temperatures by Tsao et al (54), and showed that the excess film entropies ($\Delta S^{f,ex}$) were negative and that their negativity increased with the decreasing distance separating two hydrophobic surfaces. This finding suggests that water is more structured in the intervening layer.

The ordering of surface water molecules have been supported by the sum-frequency (SF) spectra of the water on hydrophobic surfaces. Du et al. (55) showed that the SF spectra of the interfacial water on the silica surfaces coated with octadecyltrichlorosilane (OTS) were similar to that of ice. Also, the water on the OTS-coated silica surface showed a prominent peak at 3,700 cm^{-1}, which is due to the dangling (or free) OH groups oriented at the interface. This peak, which is considered as a signature of hydrophobicity, was also observed at the air/water and air/hexane interfaces.

Eriksson et al. (48) presented a mean-field theory based on a square-gradient assumption to account for the enhanced structure rearrangement for water at the vicinity of a hydrophobic solid surface. They had the following premises:

i) A homogeneous and smooth hydrophobic solid surface.

ii) A favorable free-energy decrease associated with the molecular reorganization of the first layer of water molecules in contact with the hydrophobic surfaces due to increased number of hydrogen bonds.

iii) In a cooperative manner, the surface-induced hydrogen bond formation propagates towards the core of the thin film, resulting in a somewhat larger average number of hydrogen bonds per water molecule in the film than in the

bulk. The imposed hydrogen-bond network formation leads to an unfavorable free-energy increase throughout the core of the thin film.

The above-mentioned free energy changes are accounted for by using a dimensionless order parameter *s*(x), which is a measure of the local increase of the free energy density in the thin water film as compared to a corresponding infinite thick water film.

Eriksson et al (48) assumed that the final equilibrium state of the thin water film sandwiched between two hydrophobic surfaces is reached in a step-wise fashion: i) starting from a thin film cut out of the bulk state, the first step involves establishing the proper molecular interactions at hydrocarbon/water interfaces while retaining the average spherical-symmetric orientation of all the water molecules in the film; ii) the second step implies a change of the packing and of the average orientation of the water molecules in each of the first molecular layers next to the hydrophobic surfaces, to yield a less dense and more ordered molecular state with an increased number of hydrogen bonds and a preference for tangential alignment of the HOH bisectors of the water molecules. The film tension attained after these first two equilibration steps was denoted by γ_0^f; iii) the third step comprises a reorganization of the hydrogen-bond network throughout the film, whereby the parameter *s* becomes a function of the *x* coordinate and the final equilibrium value of γ^f is reached.

They used an approach close to the square gradient approximation to express the above-mentioned model features as follows:

$$\gamma^f = \gamma_0^f - as_0 + \int_{-h/2}^{h/2} [c_2 s^2 + c_3 (ds/dx)^2] dx \qquad [1.22]$$

The second term on the r. h. s. of this expression (where *a* is a constant) accounts for an assumed linear free energy reduction due to changing the order parameter s_0 for the water layers in direct contact with the hydrophobic surfaces, whereas the integral accounts for the free energy expense associated with structuring the core of the thin water film. Note in particular, that including the squared gradient term is essential as it furnishes a mechanism of energetic coupling between successive layers of water molecules. Eriksson et al. (56) further explained the physical meaning of the constants involved in the above equation: i) c_2, accounting for the free energy rise due to having more ordered local states within the core of the film than in bulk water; and ii) c_3, accounting for the free energy rise due to order parameter gradients, than in turn are likely to be linked to the co-operative aspects of hydrogen-bond formation in small clusters of water molecules.

Minimizing the film tension γ^f with respect to the order parameter function, *s*(x), yields the Euler condition

$$\frac{d^2 s(x)}{dx^2} - \frac{2c_2}{c_3} s(x) = 0 \qquad [1.23]$$

The above equation should be solved taking into account the proper boundary conditions: s(-h/2) = s(h/2) = s_0, corresponding to the interaction between two hydrophobic surfaces. The solution is thus given by:

$$s(x) = \left(\frac{a}{2c_3 b} \right) \frac{\cosh(bx)}{\sinh(bh/2)} \qquad [1.24]$$

and

$$\gamma^f(h) = \gamma_0^f - \left(a^2/4c_3b\right)\coth(bh/2) = \gamma_0^f - as_0/2 \\ = \gamma_0^f - \left(B/2\pi\right)\coth(bh/2) \quad [1.25]$$

The constant b stands for the quotient $\sqrt{2c_2/c_3}$, while the interaction constant B equals $\pi a^2/\sqrt{8c_2c_3}$.

For infinitely large film thicknesses, the film tension lowering is given by:

$$\gamma^f(h=\infty) - \gamma_0^f = -B/2\pi \quad [1.26]$$

By taking the difference between Eq. [1.25] and Eq. [1.26] and making use of the Derjaguin approximation, one finds that the hydrophobic attraction force as measured by means of a surface force apparatus with cylindrically shaped hydrophobic surfaces having radii equal to R, is given by the expression:

$$F/R = 2\pi\Delta\gamma^f = -B[\coth(bh/2) - 1] \quad [1.27]$$

$$\Delta\gamma^f = -\int_{H=\infty}^{H} \Pi_{hb} dH \quad [1.28]$$

For two parallel-plane air/water interfaces, the corresponding hydrophobic force Π_{hb} of surface-induced water structure origin can be derived from combining Eqs. [1.27] and [1.28]:

$$\Pi_{hb} = -\frac{bB}{2\pi}[\coth^2(bH/2) - 1] \quad [1.29]$$

where H_e is the equilibrium film thickness, b^{-1} is set equal to 15.8 nm, and B is a constant representing the strength of the hydrophobic force.

Eriksson et al. (56) generalized their water-structure-based, quasi-thermodynamic theory and successfully applied it to explain the experimental data recorded by Claesson et al. (57). It was observed that the hydrophobic force in asymmetric aqueous films between hydrophobized mica/bare mica surfaces are smaller than in symmetric aqueous films between two hydrophobized mica surfaces.

Returning to the question as to how the hydrophobic force decays with the distance separating two macroscopic particles, Laskowski and Kitchener (58) suggested that "the multimolecular water layer on the surface of a hydrophobized silica is unstable, which is ascribed to a less favorable state of molecular association at a certain distance from the surface than in normal (bulk) water". These investigators were the first to recognize the existence of a long-range non-DLVO hydrophobic force and to suggest that the long-range character arises from the structural properties of water. Similarly, Derjaguin et al. (59) referred to the hydrophobic attraction in terms of the "structure component of the disjoining pressure".

Recent studies showed that air bubbles may be hydrophobic (39, 55), thus raising the question whether hydrophobic force serves as the major driving force for fast bubble

coalescence observed in pure water. To a larger extent, is the water structure mechanism supported by surface force data for foam films?

Bergeron (28) found the discrepancy between DLVO theory and foam film disjoining pressure data, and he suggested that it may originate from hydrophobic interactions. Likewise, Bergeron proposed the presence of hydrophobic force in pseudoemulsion (air-water-oil) films. The nature of the hydrophobic force in these films was not known yet.

The role of hydrophobic force in bubble coalescence was first proposed by Craig et al (60), recognizing that gas bubbles are highly hydrophobic in view of high interfacial tension of air/water interface (72 mN/m). Similarly, Deschenes et al (61) measured the hydrophobicity of various gases by means of bubble coalescence. Tchaliovska, et al (30), measured equilibrium film thickness of dodecylammonium hydrochloride (DAH) using the thin film pressure balance (TFPB). From the equilibrium film thickness, they calculated the electrical surface potential based on the DLVO theory. Then they compared the DLVO-predicted surface potentials to those calculated from surface tension data using the Gibbs adsorption isotherm. The results obtained from these two approaches did not agree with each other, implying that there might be the hydrophobic attractive force in foam films.

Further, Yoon and Aksoy (62) measured the equilibrium thicknesses (H_e) of the thin foam films stabilized by dodecylammonium hydrochloride (DAH) and quantified the hydrophobic force in DAH-stabilized films. As discussed in the forgoing section, hydrophobic force may play a role in foam films, in which case the DLVO theory can be extended as follows:

$$\Pi = \Pi_{el} + \Pi_{vw} + \Pi_{hb} \qquad [1.30]$$

to include contributions from hydrophobic force (Π_{hb}), which may be expressed as a power law:

$$\Pi_{hb} = -\frac{K_{232}}{6\pi H^3} \qquad [1.31]$$

where H is film thickness and K_{232} is a constant. An advantage of using Eq. [1.23] rather than an exponential form is that it is of the same form as the van der Waals' pressure. Therefore, K_{232} can be directly compared with the Hamaker constant A_{232}.

When using the thin TFPB technique to measure the thickness of a film (2, 63, 64), the disjoining pressure of a soap film should be equal to the capillary pressure (P_c) at equilibrium. Thus,

$$\Pi = P_c \ , \qquad [1.32]$$

where P_c is the capillary pressure at the meniscus of a horizontal film (2, 64) and is given by

$$P_c = \frac{2\gamma}{R_c} \ , \qquad [1.33]$$

where γ is surface tension, and R_c is the inner radius (=2 mm) of a film holder.

Substituting Eqs. [1.15], [1.19], [1.29] and [1.30] into Eq. [1.31], Yoon and Aksoy reached the following equation:

$$64C_{el}RT\tanh^2\left(\frac{ze\psi_s}{4kT}\right)\exp(-\kappa H_e)-\frac{A_{232}}{6\pi H_e^{\,3}}-\frac{K_{232}}{6\pi H_e^{\,3}}-\frac{2\gamma}{r_c}=0\,, \qquad [1.34]$$

in which H_e is the equilibrium thickness. Yoon and Aksoy calculated the double-layer potential (ψ_s) at the Stern plane by first calculating the adsorption density (Γ_+) of the ionic surfactant at the air/water interface, which in turn was used to calculate the surface potential (ψ_0) using the Gouy-Chapman theory. The surface potential was then corrected for the adsorption of counter ions at the air/water interface using the Stern model. Equation [1.34] can be solved for K_{232} using the values of H_e determined experimentally and the value of ψ_s obtained in the manner described above, and the Hamaker constant (A_{232}) from literature. Israelachvili (65), for example, gave the value of A_{232}=3.7x10^{-20} J. One should note here that at low surfactant concentrations, the choice of A_{232} does not make a big difference in the calculation of K_{232} using Eq. [1.34] because the latter is much larger than the former.

Yoon and Aksoy's results show that at low surfactant concentrations there is hydrophobic force in foam films and its strength decreases with increasing surfactant concentration. The hydrophobic force can be up to two orders of magnitude larger than the van der Waals force.

Another way to detect hydrophobic force in foam films has been carried out by Angarska et al. (33). As the thickness of a foam film is reduced by drainage, the film ruptures catastrophically when the thickness reaches a critical thickness (H_{cr}). It is believed that, a film surface is always in thermally- or mechanically-induced oscillation, causing the instantaneous distance between the two interfaces in a foam film to be smaller than the measured distance. The amplitude of the oscillation increases, when the instantaneous distance between the two surfaces is within the range of an attractive force, i.e., van der Waals force. When the distance between the two surfaces reaches H_{cr}, the film ruptures spontaneously.

If a foam film ruptures at the H_{cr} predicted by the capillary wave model, there is no need to invoke the hydrophobic force. Indeed many investigators showed that in the absence of repulsive forces, the model can predict the critical rupture thicknesses (66-69). Recently, Angarska *el al.* (33) showed that the predictions of the model developed by Valkovska et al. (69) were in good agreements with the experimental data obtained by Manev el al. (70). Note, however, that the rupture thicknesses were measured at high concentrations of SDS (4.3x10^{-4} M) and NaCl (0.25 M), under which conditions the air/water interface becomes hydrophilic.

Angarska et al. (33) showed, however, that the capillary wave model fails at low SDS concentrations. The H_{cr} values measured at 0.5-, 1.0-, and 10x10^{-6} M SDS and 0.3 M NaCl concentrations at different film radii deviated from those predicted by the capillary wave model without considering the contributions from hydrophobic force. At 1x10^{-6} M, the experimental values of H_{cr} were substantially larger than predicted by the capillary wave model derived by assuming that the disjoining pressure due to hydrophobic force (Π_{hb}) was zero. At 10^{-5} M, the discrepancy was much reduced;

however, the experimental values were still considerably higher than predicted. Angarska *et al.* (33) used Eq. [1.29] to represent the hydrophobic force where the parameters *B* and b^{-1} represent the strength and decay length of the hydrophobic force, respectively. By assuming that b^{-1}= 15.8 nm at all SDS concentrations studied, Angearska et al. back-calculated the values of *B* to be 0.656, 0.471, and 0.0334 $\mu J/m^2$ at 0.5-, 1.0-, and $10x10^{-6}$ M SDS, respectively, and at 0.3 M NaCl. These results suggest that hydrophobic force decreases with increasing surfactant concentration. It should be noted here that the hydrophobic forces obtained by these investigators were very small, even smaller than the van der Waals forces.

Hydration Force

The hydration force is a short range solvation force in extremely thin aqueous film. It originates from molecular ordering at the interface (35). Jönsson and wennerström (70) explained the hydration force with the solvation of highly polar surface groups. The hydration force may be responsible for the stability of NBFs.

According to Eriksson et al. (48), the equations [1.23] can be solved taking into account the proper boundary conditions: s(-h/2) = -s(h/2) = s_0, corresponding to the interaction between two hydrophilic surfaces. The order parameter function is thus given by:

$$s(x) = \left(\frac{a}{2c_3 b} \right) \frac{\sinh(bx)}{\cosh(bh/2)} \qquad [1.35]$$

and

$$\gamma^f(h) = \gamma_0^f - \left(a^2 / 4c_3 b \right) \tanh(bh/2) \qquad [1.36]$$

where the constant *b* stands for the quotient $\sqrt{2c_2/c_3}$.

Likewise, by taking the difference in film tension between thin film and infinitely thick film and making use of the Derjaguin approximation one finds that the hydration force as measured by means of a surface force apparatus with cylindrically shaped hydrophobic surfaces having radii equal to *R,* can be given by the expression:

$$F/R = 2\pi\Delta\gamma^f = -\frac{\pi a^2}{2c_3 b}[1 - \tanh(bh/2)] \qquad [1.37]$$

Undulation Force

The undulation force develops from the undulations of membranes approaching each other. The concept of the repulsive forces caused by out-of-plane undulations between lipid bilayers was first introduced by Helfrich and his coworkers (72). It is accepted that the undulation repulsion is a kind of steric force, arising from the entropic confinement of thermally excited undulation of the bilayers by neighboring bilayers (73). The undulation force is of long-range nature, as compared to hydration force and other short-ranged forces. A general expression for the undulation force can be given as

$$P_{und}(D) \propto \frac{(kT)^2}{K_b D^3} \qquad [1.38]$$

where D is the mean separation distance between two bilayers, kT is the thermal energy, and K_b is the elastic bending modulus.

More recently, a new expression is given by Walz and Ruckenstein (73):

$$P_{und}(D) = C\frac{(kT)^2}{K_b (D-\delta)^3} \qquad [1.39]$$

where δ corresponds to a distance of closest approach, about 2 nm (74), K_b is the elastic bending modulus, usually within the order of kT (=4.1x10^{-21} J) (75), and C is the adjustable parameter, around 0.06 (76).

1.4 Dissertation outline

This dissertation combines fundamental measurements of surface forces in foam films with the stability of three-dimensional foams. Throughout this work, basically two methods were used. One is the static method; the other, dynamic methods. The static method is to measure equilibrium film thickness and disjoining pressure, which are analyzed by the DLVO theory with electrical surface potential as the other important parameter. The dynamic methods were employed primarily to detect the hydrophobic force in foam films at high electrolyte concentrations. The Reynolds lubrication theory was used to analyze the measured rate of film thinning.

Chapters 2 and 3 deal with foam films and foams stabilized by an ionic surfactant, sodium dodecyl sulfate (SDS). Chapters 4 and 5 deal with foam films and foams stabilized by a nonionic surfactant, methyl isobutyl carbinol (MIBC). Chapter 6 describes the effect of pH on surface forces in surfactant-free foam films. Chapter 7 deals primarily with a comparison between the stability of a single foam film and three-dimensional foams stabilized by various common frothers (pentanol, octanol, MIBC, and PPG). The formulas of these reagents are given in Table 1.1.

Table 1.1 Chemical formulas of reagents.

Sodium Dodecyl Sulfate (SDS)	$H(CH_2)_{12}O\ SO_3^-Na^+$
n-pentanol	$C_5H_{11}OH$
n-octanol	$C_8H_{17}OH$
Methyl Isobutyl Carbinol (MIBC) or 4-methyl-2-pentanol	$(CH_3)_2CHCH_2CH(OH)CH_3$
Polypropylene glycol (PPG) with average M.W. 400	$H[OCH(CH_3)CH_2]_nOH$

1.5 References

1. Scheludko, A., *Kolloid Z.*, 191 (1963) 52.
2. Scheludko, A., *Advances in Colloid and Interface Sci*. 1 (1967) 391.
3. Malhotra, A.K. and Wasan, D.T., in: I.B. Ivanov (Ed.), Thin Liquid Films, Surfactant Science Series, 29 (1988) 829.

4. Graciaa, A., Creux, P., and Lachaise, J., in A. V. Delgado (Ed.), Interfacial Electrokinetics and Electrophoresis, Surfactant Science Series, volume 106, Marcel Dekker, Inc., New York, 2002, pp 825.
5. McTaggart, M.A., *Philos. Mag*, 44 (1922) 386.
6. Alty, T., *Proc. R. Soc. London Ser. A* 106 (1924) 315.
7. Yoon, R-H. and Yordan, J. L., *J. Colloid Interface Sci*., 113 (1986) 430.
8. McShea, J.A., and Callaghan, I.C., *Colloid Poly. Sci*. 261 (1983) 757.
9. Usui, S., and Sasaki, H., *J. Colloid Interface Sci*. 65 (1978) 36.
10. Collons, G.L., Motarjemi, M., and Jameson, G.L., *J. Colloid Interface Sci*. 63 (1978) 69.
11. Fukui, Y., and Yuu, S., *AICHE J*. 28(5) (1982).
12. Kubota, K., Hayashi, S., and Inoaka, M., *J. Colloid Interface Sci*. 95 (1983) 362.
13. Manev, E, and Pugh, R J, *Langmuir,* 7 (1992) 2253.
14. Bergeron*,* V, Watermo, Å, and Claesson, P M, *Langmuir* 12 (1996) 1336.
15. Karraker, K A, and Radke, C J, *Advances in Colloid and Interface Sci,* 96 (2002) 231.
16. Stubenrauch, C., and Klitzing, R., *Journal of Physics: Condensed Matter,* 15 (2003) R1197.
17. Currie, B. W., and Alty, TV., *Proc. R. Soc. London Ser. A*, 120 (1930) 622.
18. Vassilev, P., Hartnig, C.H., Koper, M.T.M., Frechard F. and van Santen, R.A., *J. Chem. Phys*. 115 (2001) 9815.
19. Lee, B., Justus, L. Lee, J.W. and Greebaum, E., *J. Phys. Chem. B* 107 (2003) 14225.
20. Lyklema J, and Mysels, K.J., *J. Am. Chem. Soc.* 87 (1965) 2539.
21. Bélorgey O. and Benattar, J.J., *Physical Review Letters* 66 (1991) 313.
22. Sentenac D. and Dean, D.S., *J. Colloid Interface Sci*., 196 (1997) 35.
23. Bergeron, V., *J. Phys., Condensed Matter* 11 (1999) R215.
24. Israelachvili J. N. and Wennerström H., *J. Phys. Chem.* 96 (1992) 520.
25. Derjaguin B.V. and Churaev, N.V., *J. Colloid Interface Sci*., 66 (1978) 389.
26. Eriksson J.C. and Toshev, B.V., *Colloids and Surfaces*, 5(1982) 241-264.
27. de Feijter, J.A., in: I.B. Ivanov (Ed.), Thin Liquid Films, Surfactant Science Series, volume 29, 1988, pp 1.
28. Exerowa, D., Kolarov, T., and Kristov, K.H.R., *Colloids and Surfaces,* 22 (1987) 171.
29. Bergeron, V., PhD thesis, University of California at Berkeley, 1993.

30. Tchaliovska, S.; Manev, E.; Radoev, B.; Eriksson, J. C.; Claesson, P. M. *J. Colloid Interface Sci.* 168 (1994) 190.

31. Sedev, R., Németh, Zs., Ivanova, R., and Exerowa, D., *Colloids Surfaces A* 149 (1999) 141.

32. Ruckenstein E. and Bhakta, A., Langmuir, 12 (1996) 4134.

33. Angarska, J. K., Dimitrova, B. S., Danov, K. D. Kralchevsky, P. A., Ananthapadmanabhan, K. P., and Lips, A., *Langmuir* 20 (2004) 1799.

34. Churaev, N.V., *Advances in Colloid and Interface Sci.* 114–115 (2005) 3.

35. Israelachvili, J N, *Intermolecular and surface forces with Applications to Colloid and Biological Systems,* Academic Press, Orlando, Fl., 1985.

36. Graciaa, A. Morel, G. Saulner, P. Lachaise J. and Schechter, R.S., *J. Colloid and Interface Sci*., 172 (1995) 131.

37. Hamaker, H.C., *Physica*, 4 (1937) 1058.

38. Lifshitz, E.M., *Zhur. eksp. teor. Fiz*., 29, 94 (1955).

39. Yoon, R.-H.; Yordan, J. L. *J. Colloid Interface Sci.* 146 (1991) 565

40. Blake, T. D.; Kitchener, J. A., *J. Chem. Soc. Faraday Trans*. 68 (1972) 1435.

41. Israelachvili, J.N. and Pashley, R. *Nature*, 300 (1982) 341.

42. Rabinovich, Ya, I,; Derjaguin, B. V., *Colloids and Surfaces* 30 (1988) 243.

43. Claesson, P.M. and Christenson, H.K., *J. Phys. Chem*. 92 (1988) 1650.

44. Rabinovich Y.I. and Yoon, R.-H., Langmuir, 10 (1994) 1903.

45. Meyer, E.E., Liu, Q., and Israelachvili, J.N., *Langmuir* 21 (2005) 256-259.

46. Lin, Q., Meyer, E.E., Tadmor, M., Israelachvili, J. N. And Kuhl, T., *Langmuir*, 21 (2005) 251.

47. Zhang, J., Yoon, R.-H., Mao, M. and Ducker, W.A., *Langmuir*, 21 (2005) 5831.

48. Eriksson, J. C., Ljunggren S., Claesson, P. M., *J. Chem. Soc., Faraday Trans*. 2, 85 (1989) 163.

49. Parker, J. L.; Claesson, P. M.; Attard, P.; *J. Phys. Chem*., 98 (1994) 8468.

50. Craig, V. S. J., Ninham, B. W., Pashley, R. M., *Langmuir* 14 (1998) 3326.

51. Mao, M., Zhang, J., Yoon, R.-H., Ducker, W. A., *Langmuir* 20 (2004) 1843.

52. Israelachvili, J.N., McGuiggan, P.M., *Science* 241 (1988) 795.

53. Eriksson, J.C., and Yoon, R.-H., in: M.C. Fuerstenau, (Ed.), Flotation Handbook. Society of Mining Engineers, Golden, Colorado, in press.

54. Tsao, Y., Yang, S. X., Evans, D. F., Wennerström, H., *Langmuir* 7 (1991) 3154.

55. Du, Q., Freysz, E., Shen, Y. R., *Science* 264 (1994) 826

56. Eriksson, J.C., Henriksson, U., Kumpulainen, A., *Colloids and Surfaces A*, in press.

57. Claesson, P.M., Herder, P.C., Blom, C.E., Ninham, B.W., *J. Colloid Interface Sci*. 118 (1987) 68.

58. Laskowski, J., Kitchener, J.A., *J. Colloid Interface Sci.* 29 (1969) 670.

59. Derjaguin, B.V., Churaev, N.V., and Muller, V.M., Surface Forces, Consultants Bureau, New York, 1987.

60. Craig, V.S.J.; Ninham, B.W.; Pashley, R.M., *J. Phys. Chem.* 97 (1993) 10192.

61. Deschenes, L., Zilaro, A P, Muller, L J, Fourkas, J T, and Mohanty U, *J Phys. Chem.* 101 (1997) 5777.

62. Yoon, R.-H., and Aksoy B.S., *J Colloid Interface Sci,* 211 (1999) 1.

63. Scheludko, A., Exerowa, D., *Comm. Dept. Chem., Bul. Acad. Sci.*, 7 (1959) 123.

64. Exerowa, D., Kruglyakov, P. M., *Foam and Foam Films*, Elsevier, 1998.

65. Israelachvili, J N, *Intermolecular and surface forces*, Academic press: London, 1992.

66. Radoev, B. P., Scheludko, A. D., Manev, E. D., *J. Colloid Interf. Sci*., 95 (1983) 255.

67. Vrij, A., *Discuss. Faraday Soc*. 42 (1966) 23.

68. Vrij, A., Overbeek, J. Th. G., *J. Am. Chem. Soc*. 90 (1968) 3074.

69. Valkovska, D.S., Danov, K.D., Ivanov, I.B., *Adv. Colloid Interf. Sci*. 96 (2002) 101.

70. Manev, E.D., Sazdanova, S.V., Wasan, D.T., *J. Colloid Interf. Sci*. 97 (1984) 591.

71. Jösson, B. And Wennerström, H., *J. Chem. Soc, Faraday Trans.* 2, 79 (1983) 19.

72. Harbich, W., Servuss, R.M., Helfrich, W., *Phys. Lett.* 57A (1976) 294.

73. Walz, J.Y. and Ruckenstein, E., *J. Phys. Chem. B* 103 (1999) 7461.

74. Servuss, R.M. and Helfrich, W. J. Phys. Fr. 50 (1989) 809.

75. Safinya, C.R., Roux, D., Smith, G.S., Sinha, S.K., Dimon, P., Clark, N.A. and Bellocq, A.M., *Physical review letters* 57 (1986) 2718.

76. Janke, W. and Kleinert, H., *Phys. Lett. A*. 117 (1986) 353.